American Mineralogist, Volume 75, pages 983–991, 1990

Far infrared, X-ray powder diffraction, and chemical investigation of potassium micas

Paul A. Schroeder
Department of Geology and Geophysics, Yale University, P.O. Box 6666, New Haven, Connecticut 06511, U.S.A.

Abstract

Naturally occurring potassium micas with a range of composition have been examined employing the analytical techniques of far infrared (IR) spectroscopy, X-ray powder diffraction (XRD), and major oxide and F analysis. Structure parameters predicted by geometric models, including torsional mode interlayer frequency (ν_i), d value (d_{001}), and b cell parameter are compared with those determined from structural refinement of potassium micas of similar composition. Differences are likely the result of assumptions inherent in the geometric models, including the frequency of the interlayer mode as a proxy for the K inner-O bond distance and the constancy of the combined octahedral-tetrahedral sheet thickness. Study of the IR, XRD, and chemical parameters shows the following relationships: (1) Solid solution of OH and F in trioctahedral structures significantly affects torsional vibrational modes, with increasing frequency correlating with increasing F. (2) Heating-induced dehydroxylation of dioctahedral species and heating-induced oxidation of Fe^{2+} trioctahedral species provide strong evidence that OH-orientation controls the frequency of the interlayer torsional mode. (3) Multivariate statistical analysis of potassium-mica intralayer sheet composition and the frequency of the interlayer torsional mode reveals a strong correlation between the vibrational frequency of the K interlayer torsional mode and octahedral sheet composition. The following preliminary formula is presented, assuming 22 O equivalents per unit formula:

$$\nu_i\ (\mathrm{cm}^{-1}) = 79.6 + 0.96\mathrm{Mg}^{2+} - 4.23\mathrm{Fe}^{2+} + 7.61\mathrm{Al}^{3+} + 9.09\mathrm{Fe}^{3+} - 4.65\mathrm{Li}^{+} + 2.20\mathrm{F}^{-}.$$

The frequency of the interlayer torsional mode directly reflects the tetrahedral sheet environment. This relationship therefore supports previous suggestions, based on XRD data alone, that the sheet dimensions and distortions of phyllosilicates are controlled largely by the composition of the octahedral layer. (4) Multiple-mode behavior provides evidence for the presence of compositionally different octahedral cation sites within a given structure. However, absorption spectra alone do not provide information about ordering of the octahedral environments.

Introduction

Interrelationships between structural and chemical parameters of coarse-grained phyllosilicates have been derived traditionally from the combined analysis of single-crystal X-ray diffraction data and major oxide compositions. In contrast, characterization of the physical and chemical states of fine-grained micas often relies on integrating data obtained from a variety of techniques, including X-ray powder diffraction (XRD), infrared (IR) spectroscopy, and nuclear magnetic resonance (NMR) spectroscopy. Studies of near- and mid-IR mica absorption spectra have provided insight into the causes of vibrational modes of OH, alumino-silicate tetrahedra, and metal octahedra, which have helped to constrain the locations and orientations of these intrasheet components (e.g., Farmer, 1974). More recently, the advent of the Fourier-transform infrared spectrometer has made possible routine measurement of absorption spectra in the far-IR frequency range of 300–50 cm^{-1}. This is a region where the calculation of normal modes from quantitative modeling of vibrational spectra of 2:1 phyllosilicates predicts four fundamental, infrared-active, interlayer vibrational modes and where absorption bands are observed (Ishii et al., 1967).

The relative importance of octahedral and tetrahedral charge and mass variations on interlayer vibrational modes has been discussed by several authors, including Farmer (1974), Tateyama et al. (1977), Velde (1978), Roth (1978), Fripiat (1982), and Velde and Couty (1985). However, to date, with the exception of Prost and Laperche (1990), no consistent relationships have been found. The purpose of this paper is to assess the effect of octahedral and tetrahedral substitutions on the interlayer absorption bands of potassium micas.

0003–004X/90/0910–0983$02.00

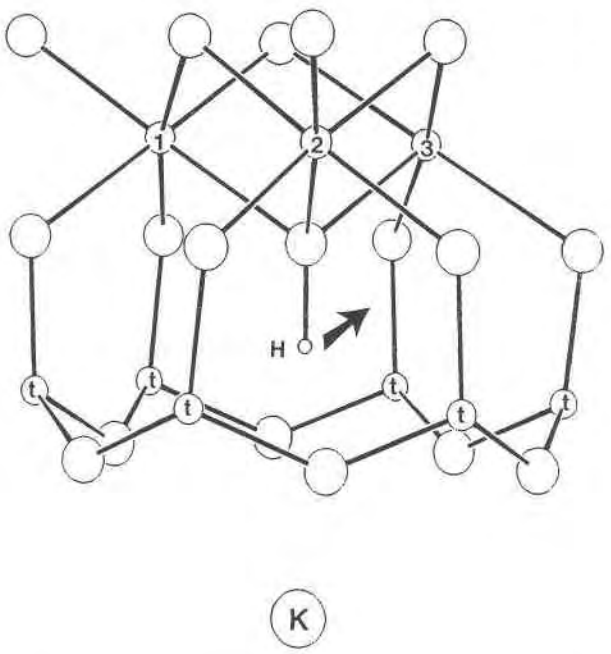

Fig. 1. Schematic diagram of a portion of the trioctahedral 2:1 layer structure showing the locations of octahedral cations (1, 2, 3), tetrahedral cations (t), OH proton (H), and interlayer cation (K). Arrow indicates change in orientation of H upon heating-induced oxidation of Fe^{2+}.

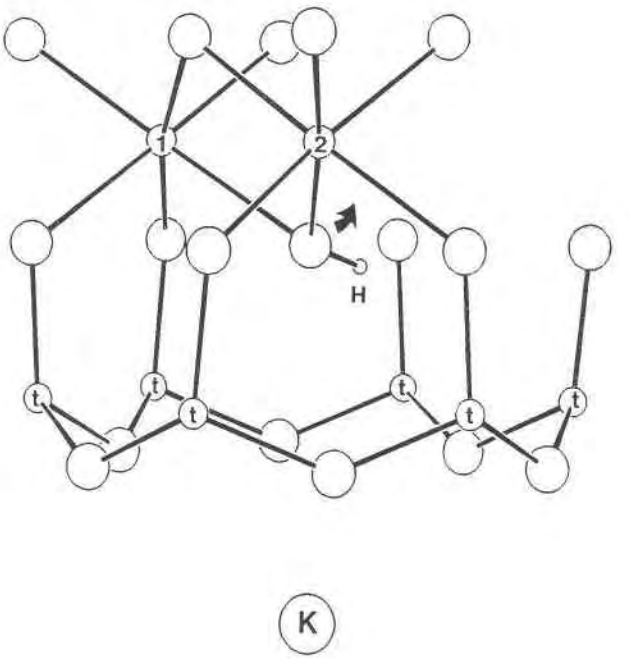

Fig. 2. Dioctahedral 2:1 layer structure showing the locations of octahedral cations (1,2), tetrahedral cations (t), OH proton (H), and interlayer cation (K). Arrow indicates relocation of hydroxyl O toward the octahedral metal sheet upon heating-induced dehydroxylation.

Structural relationships and previous work

The nature of the interlayer absorption-band region is generally thought to be controlled by the charge and mass distribution of the chemical components both between and within individual layers (Farmer, 1974). More precisely, these components can be grouped according to the (1) interlayer cation, (2) di- and trioctahedral cations, (3) tetrahedral Si and Al cations, and (4) OH and F. The effects of intralayer cation components (items 2 and 3 above) on sheet dimensions were first described by Radoslovich (1962), who observed a relationship between the measured *b*-cell parameter and octahedral sheet composition based on statistical analysis. Radoslovich and Norrish (1962) further pointed out the importance of octahedral composition in controlling the overall structure of phyllosilicates.

The symmetry of the tetrahedral basal O cavity (i.e., the interlayer cation site) is primarily related to the distortion of the tetrahedral sheet. This distortion occurs largely in response to lateral misfit with the octahedral sheet. Departure of the hexagonal network from the ideal angle of 120° is defined by the angle α and serves as a convenient parameter to monitor the amount of tetrahedral sheet distortion. The *b*-cell parameter is generally reflected in α, but the misfit is relative and does not necessarily correspond to the absolute dimensions of the sheets. The resultant ditrigonal symmetry of the basal O atoms forms a set of nearest neighbor inner and a set of next-nearest neighbor outer interlayer bonds between cations and O atoms. Potassium-mica bonds are hereafter referred to as $K\text{-}O_{inner}$ and $K\text{-}O_{outer}$ bonds, respectively.

The charge and mass of the interlayer cation also can influence the symmetry of the ditrigonal cavity. Cations with large ionic radii (e.g., Cs^+) may prop open the ditrigonal cavity and limit articulation of the basal O cage. These tetrahedral distortions further translate to the octahedral sheet. Leonard and Weed (1967), Suquet et al. (1975), and Eirish and Tret'yakova (1970) have shown that dioctahedral vermiculite and montmorillonite exhibit measurable variation in *b* with exchange of cations (e.g., Li, K, and Cs) and change in hydration state. The relative contribution of interlayer cations to sheet distortion, compared to that of octahedral misfit, is considered small but may be important when considering cations with large ionic radii.

Orientation of the vector between the proton and O of the central OH group is largely influenced by octahedral cation occupancy, depending upon vacancies or charge asymmetries within the sheet (Vedder and MacDonald, 1963; Giese, 1971). It is well known that in trioctahedral structures O-H bonds typically are oriented nearly perpendicular to the *ab* plane and are positioned in the center of the ditrigonal tetrahedral cavity (Fig. 1). For dioctahedral potassium micas, O-H bonds on average are inclined 10° to 20° to the **ab** plane, toward the vacant octahedral metal site (Fig. 2). As a result of these different orientations a significant range in repulsion effects can

occur between the proton of the OH and the interlayer K.

Tateyama et al. (1977) were the first to suggest that the frequency of the strong absorption band observed in the 110–70 cm^{-1} region of potassium micas is a function of the bond length between K and the basal inner O of the ditrigonal cavity. Using 15 potassium micas, they determined a linear correlation between the frequencies and the K-inner O bond lengths of compositionally similar potassium micas. Their least-squares fit is given as

$$K\text{-}O_{inner} = 3.676 - 0.0076\nu_i \qquad R^2 = 0.94, \qquad (1)$$

where $K\text{-}O_{inner}$ is the bond length (Å) and ν_i is the observed wavenumber (cm^{-1}) that they ascribed to the $K\text{-}O_{inner}$ absorption band. The equation shows the relation of increasing frequency with shorter $K\text{-}O_{inner}$ distances. Unfortunately, the fit is biased by the fact that only seven absorption frequencies were measured. Those seven measured values were assigned to the eight other potassium micas based on similarities in composition (e.g., a synthetic F-rich phlogopite was assigned the same frequency as natural phlogopite). Six of the directly measured absorption frequencies of Tateyama et al. (1977) appear in Figure 3 as solid circles.

Tateyama et al. (1977) further developed an expression for calculating the amount of tetrahedral rotation (Eq. 2). Assuming a constant T-O-T thickness and trigonometric relationships established by Franzini (1969) and McCauley and Newnham (1971) then

$$\alpha = \arctan\left(\sqrt{3} - \frac{6\sqrt{K\text{-}O_{inner}^2 - 0.25(d_{001} - 6.642)^2}}{b}\right), \qquad (2)$$

where d_{001} is the interplanar spacing and b is the unit-cell parameter, both in Å. The potential ability to predict α from relatively simple IR and XRD measurements presents a useful way to characterize the structural state of true potassium micas and possibly their lower-layer charge counterparts, illite and K-saturated smectite. Testing the soundness of these models is therefore important to ascertain if this method of determining α is valid.

Assignments of the vibrational modes to the absorption bands observed in the region of 300–50 cm^{-1} have been primarily based on a theoretical treatment of the 2:1 sheet components using group theory and potential energy functions to model vibrational spectra (Ishii et al., 1967; Loh, 1973). Laperche and Prost (1989), however, using oriented single crystals and polarized IR radiation, recently have provided empirical evidence for band assignments in the energy region below 200 cm^{-1}. Dichroic absorption effects were observed in the bands of the region of 180–120 cm^{-1}, while crystals were rotated about their **c** axes. Assuming that crystal orientation is related to translational dipole moments of interlayer cation motion in the **ab** plane, these bands can be assigned to the translational modes of Ishii et al. (1967). The strong band observed in the region of 110–70 cm^{-1} shows no dichroic

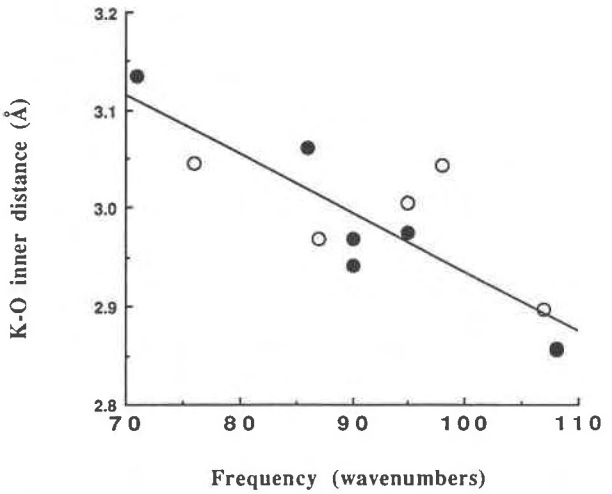

Fig. 3. Measured K interlayer absorption frequencies compared with $K\text{-}O_{inner}$ distances from structurally refined potassium micas of similar composition. Solid circles are measured frequencies of natural potassium micas after Tateyama et al. (1977). Open circles are measured potassium mica frequencies from this study.

effects, suggesting it is due to a torsional motion involving basal O vibrations relative to the interlayer cation. This latter band is equivalent to the frequency that Tateyama et al. (1977) referred to as ν_i and will be the focus of all subsequent discussion.

The effects of the charge and mass of the interlayer cation on what is now believed to be the interlayer torsional mode have been discussed by Fripiat (1982) and Laperche and Prost (1989). Their observations indicate a threshold cation size, below which the cations do not establish a single equilibrium position within the ditrigonal basal O cavity of the tetrahedral sheet. Above the threshold, larger cations occupy a unique equilibrium position within the cavity, and coherent absorption results. Because of its ionic radius (1.33 Å), K^+ is well suited for study of the effects of octahedral and tetrahedral substitution on interlayer modes. It fits optimally into the basal O cavity, with a minimum of ditrigonal distortion induced by interlayer cations, while still large enough to allow for far-IR investigation.

Experimental

Frequencies of the interlayer vibrational mode (ν_i), interplanar spacings (d_{001}), b cell parameters (b), and chemical compositions of the potassium micas used in this investigation were either measured or obtained from published data for which all analyses were on the same sample.

Far-IR absorption spectra were collected using a Nicolet SX-60 FTIR spectrometer using a Mylar beamsplitter of 6 or 25 μm, Globar source, and DTGS detector. To keep grain size effects comparable, sheet micas were blended with H_2O in a mixer and then gently ground until approximately 20 μm in size. Samples were sedimented

Table 1. Chemical analyses of potassium micas

	musc*	pheng**	celad†	phlog‡	biot§
SiO_2	43.60	46.50	51.50	42.60	34.30
TiO_2	<0.01	0.15	0.07	0.81	3.49
Al_2O_3	33.80	33.30	1.60	13.80	13.80
Cr_2O_3	<0.01	<0.01	<0.01	<0.01	0.01
Fe_2O_3	1.36	<0.01	17.70	0.72	8.00
FeO	2.00	0.20	3.20	2.70	25.00
CaO	<0.01	<0.01	<0.01	<0.01	<0.01
MgO	1.72	3.72	7.82	25.70	6.70
MnO	0.16	<0.01	0.01	<0.01	0.36
K_2O	10.30	9.87	9.81	9.49	10.20
Na_2O	<0.01	<0.01	<0.01	<0.01	<0.01
P_2O_5	0.02	<0.01	0.02	<0.01	0.01
LOI	7.35	6.73	8.73	1.54	−1.57
F	0.64	0.01	0.01	3.80	0.62
Total	100.94	100.48	100.46	101.17	100.91
Number of ions on the basis of $O_{20}(OH,F)_4$					
Si	6.02	6.23	7.72	5.92	5.32
Al	1.98	1.77	0.27	2.08	2.52
Σ Tet.	8.00	8.00	8.00	8.00	7.85
Al	3.51	3.49	0.02	0.18	0.00
Ti	0.00	0.02	0.01	0.08	0.40
Fe^{3+}	0.14	0.00	2.00	0.08	0.60
Fe^{2+}	0.23	0.02	0.40	0.31	3.24
Mn	0.02	0.00	0.00	0.00	0.05
Mg	0.35	0.74	1.75	5.33	1.55
Σ Oct.	4.26	4.28	4.18	5.98	5.85
K	1.81	1.69	1.88	1.68	2.02
Tet. charge	−1.98	−1.77	−0.027	−2.08	−3.14
Oct. charge	0.17	0.08	−1.61	0.39	1.11
Int. charge	1.81	1.69	1.88	1.68	2.02
F	0.28	0.01	0.01	1.67	0.30

* Muscovite, East Morris, Connecticut.
** Phengitic muscovite, Zacapa, Guatamala (American Museum of Natural History MVJ84-52-1).
† Fe-rich celadonite, near Reno, Nevada (Yale Peabody Museum, B-6452).
‡ Phlogopite, Ottawa Co., Canada (Yale Peabody Museum, PM-7297).
§ Biotite, Russell, New York (Yale Peabody Museum, B-2972-iv).

with a density of 0.06 mg/mm² onto IR-grade silicon wafers using the technique of Schroeder (1989). Spectral resolution was set at 4 cm^{-1} with a time-averaged signal collected over 200 scans. Peak positions were reproducibly measured with precision of ±0.5 cm^{-1}.

F contents were measured using the technique of Thomas et al. (1977). Other chemical analyses were performed by XRAL Ltd., Ontario, Canada, using X-ray fluorescence for major oxides and wet chemistry for Fe^{2+} content. Cation assignments were made on the basis of 22 O equivalents per unit formula using the program Clayform (Bodine, 1987). Major oxide and structural formulae are presented in Table 1.

X-ray diffraction measurements of the d_{001} and b were made using a Scintag Pad-V diffractometer. Interplanar spacings were obtained by measurement of the position of the (005) reflection, internally calibrated with α-Al_2O_3. The α-Al_2O_3 standard was calibrated previously using NBS SRM-675. Reported spacings have an accuracy of ±0.001 Å. The (060) reflection was used to calculate b. As pointed out by previous workers (Guidotti, 1984; Frey et al., 1983), the (060) reflection cannot clearly be separated from the (3̄31) reflection. For a $2M_1$ muscovite structure, Borg and Smith (1969) calculated d values for three reflections within ±0.003 Å of the (060) spacing. Considering that the (3̄31) intensity is double that of (060) and including the contribution of $K_{\alpha 2}$ radiation, it is often difficult to clearly identify reflections. To circumvent this problem, a simple technique to gain preferred orientation of (060) has been devised and is herein described. The procedure involves settling a slurry of about 0.2 g of sample into a plastic mold of the type used for thin-section preparation. When dry, a thin coat of low-viscosity epoxy is applied and allowed to set. The epoxy sheet then is sliced into 2-mm strips, which are stacked and repotted into the plastic mold with the slices on end (i.e., perpendicular to basal spacings). The result is a preferred orientation that enhances the (060) reflection intensity. The epoxy block can be lapped to a flat surface, which minimizes sample displacement error in the diffractometer. Using an external standard, measurements are reported to ±0.005 Å. A comparison of a standard powder mount and an epoxy mount is shown in Figure 4 to illustrate the enhancement of (hk0) reflections. This method may prove generally useful in the analysis of 2:1 clay minerals.

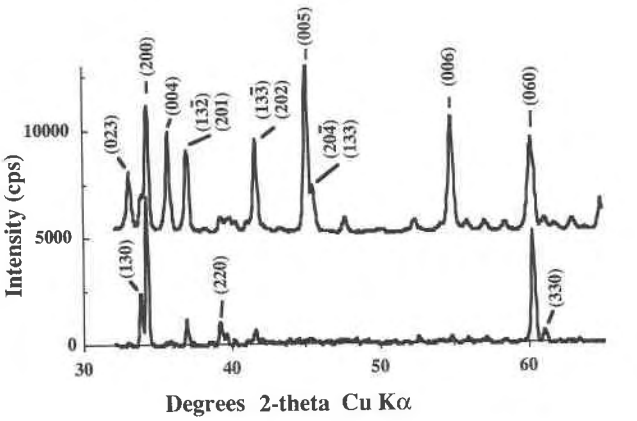

Fig. 4. X-ray diffraction patterns of the phlogopite specimen used in this study, prepared using a standard packed powder mount (upper) and epoxy preferred-orientation mount (lower). Scattering from the epoxy mount produces a broad intense peak below 30° 2θ (Cu$K\alpha$); however, higher-order reflections show enhancement of the (hk0) reflections when compared to the bulk mount.

Heating experiments were performed in an attempt to evaluate the effects of OH groups on absorption spectra. To accomplish this, samples were heated to 750 °C for several hours in a N_2-purged furnace.

Results and discussion

Far-IR absorption spectra for each potassium mica are shown in Figure 5. The torsional interlayer vibrational mode, as interpreted by Laperche and Prost (1989), is marked by the strong absorption peaks in the region of 110–75 cm^{-1}. Using K-O_{inner} distances from compositionally similar potassium micas (see Table 2 caption for references), measured absorption frequencies from this study are plotted as open circles in Figure 3. The recalculated

least-squares fit for all data yields a slope and intercept comparable to that of Equation 1; however the correlation (R^2) is much lower.

$$K\text{-}O_{inner} = 3.530 - 0.0060\nu_i \qquad R^2 = 0.72. \qquad (3)$$

Using the appropriate IR and XRD measurements for the potassium micas used in this study, α was calculated by Equation 2 (Table 2). Comparison of calculated α values with rotation angles derived from structural analysis of micas shows good agreement in some cases (e.g., muscovite) and considerable differences in other cases (e.g., celadonite). Differences are probably the result of the assumption that the vibrational mode is proxy for the $K\text{-}O_{inner}$ bond distance and the assumptions inherent in Equation 2. From these observations it is apparent that the predictive value of Equations 1 and 2 is limited, and accurate models require more complexity than originally thought.

Analysis of sheet composition

Natural potassium micas may have numerous combinations of tetrahedral and octahedral substitutions. Analysis of the effects of such substitutions on the frequency of the interlayer torsional mode can be approached in two fashions. The first approach involves varying the composition of one site while holding that of all others constant. This method can be used to assess the effect of octahedral OH and F solid solution and the effects of heating-induced changes. It is otherwise difficult to find natural potassium micas in which substitutions occur in only one structural site. Therefore, a second approach is to use multivariate statistics (Davis, 1986), which offers a way to evaluate significant relationships between ν_i and crystal chemical parameters. Each approach is discussed below.

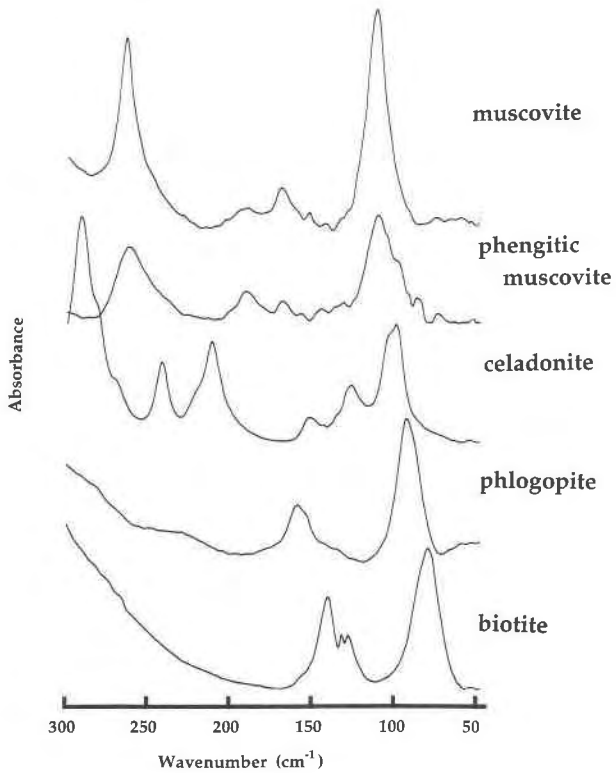

Fig. 5. Potassium mica far-IR absorption spectra for the region 300–40 cm^{-1} (see the note in Table 1 for specimen sources). Maximum absorbance value for each spectrum is about 1.5 absorbance units. Absorption in the range 125–140 cm^{-1} may be spurious owing to poor efficiency of the 25-μm beamsplitter. The phengitic muscovite spectrum was obtained using a 6-μm beamsplitter; consequently as a result of a drop in beamsplitter efficiency, absorption below 107 cm^{-1} is spurious.

TABLE 2. Lattice parameters and infrared data for potassium micas

	musc	pheng	celad	phlog	biot	F-rich phlogopite[A]
d_{001} (Å)	9.983	9.939	9.969	10.063	10.078	9.985
b (Å)	9.028	9.012	9.054(9.072)	9.216	9.312	9.185
ν_i (cm^{-1})	108	107	102(96)	87	76	95
α (°) refined	11.7[B]	9.3[C]	1.3[D]	7.5[E]	5.3[F]	6.5[G]
α (°) calc[H]	10.8	9.9	7.6	6.6	4.0	8.0
$K\text{-}O_{inner}$ (Å)	2.86	2.90	3.04	2.97	3.05	2.99
$K\text{-}O_{outer}$ (Å)	3.38	3.31	3.10	3.31	3.29	3.28
			Heated to 750 °C			
d_{001} (Å)	10.052	10.040	10.130	10.043	9.958	—
b (Å)	9.052	9.057	8.903	9.227	9.239	—
ν_i (cm^{-1})	102	103	96	90	90	—

Note: α and the K-O bond distances were taken from the same source. Parentheses in celadonite signify value of second peak observed.
[A] National Bureau of Standards SRM-675.
[B] Gatineau (1963).
[C] Sidorenko et al. (1975).
[D] Zhoukhlistov et al. (1977).
[E] Hazen and Burnham (1973).
[F] Bohlen et al. (1980).
[G] Takeda and Morison (1975).
[H] Calculated using Equation 2.

OH and F

The trioctahedral micas typically show a range of substitutions of OH for F which, because of OH orientations, makes it possible to examine the maximum effect of repulsion between K and the OH proton on the interlayer vibrational mode. Although only two members of the phlogopite OH-F series were compared in this study, the differences in frequency indicate a trend that suggests that substitutions of OH for F can be significant. A shift of the interlayer vibrational frequency from 87 cm^{-1} for phlogopite to 95 cm^{-1} for synthetic F-rich phlogopite clearly displays the effect of K-proton repulsion. The larger values of b and d_{001} of natural phlogopite when compared to synthetic F-rich phlogopite (Table 2) verify the structural results, indicating that OH in trioctahedral micas causes expansion of the lattice (Rayner, 1974; Takeda and Morison, 1975). Despite the differences in structure, the $K\text{-}O_{inner}$ and $K\text{-}O_{outer}$ distances of both phlogopite samples are quite similar. The presence of the OH proton appears to dampen the K-O vibrational frequency. With substitution of F this dampening effect is diminished. This effect accounts in part for the breakdown in the correlation between $K\text{-}O_{inner}$ and frequency originally proposed by Tateyama et al. (1977). A small amount of Fe^{2+} substitution for Mg^{2+} in phlogopite also will influence the interlayer vibrational frequency from the standpoint of mass effects (discussed below). However, it is clear that the effect of OH substituting for F appears to be of major importance.

For dioctahedral potassium micas the effect of the inclined OH orientation is to lower the repulsive force between K and the OH proton. This phenomenon is reflected in the basal d values of dioctahedral potassium micas, which are typically shorter than their trioctahedral counterparts (see, e.g., Table 2). F avoidance of Al and Fe (common dioctahedral cations), as shown by Sanz and Stone (1983), additionally maximizes the inclination of OH. The consequences of low concentrations of F in dioctahedral structures and the maximized K-O attractive forces between K and O are seen in muscovite, which has the highest observed torsional frequency (108 cm^{-1}). This observation is in full agreement with the recent work of Prost and Laperche (1990).

The effects of OH on interlayer vibrational modes can also be examined through heating experiments. Prost and Laperche (1990) were the first to report low-frequency shifts for muscovite upon heating-induced dehydroxylation. As noted by Brindley and Lemaitre (1987), there have been few complete crystallographic studies of dehydroxylated micas, and interpretations must therefore be made with caution. Not only are the effects of the OH groups lost, but the entire structure is also altered. For dioctahedral micas, the octahedral Al ions in the dehydroxylated structure change to fivefold coordination with four apical O and a residual O ion located in the Al plane (Wardle and Brindley, 1972). NMR studies of pyrophyllite dehydroxylate using ^{29}Si and ^{27}Al (Barron and Frost, 1984) indicate that whereas the integrity of the tetrahedral sheet is maintained, the nature of the octahedral sheet is uncertain. Sixfold to fivefold coordination of the Al cations in the octahedral sheet is implied only by the loss of octahedrally resonant Al. A general model of fivefold cation coordination is assumed, although the lack of NMR evidence for fivefold coordinated Al is perplexing. In dehydroxylated dioctahedral potassium micas the movement of the hydroxyl O away from the interlayer cation (Fig. 2) reduces the net K-O attractive forces. These structural changes are reflected in muscovite-dehydroxylate by the lengthening of the values of interplanar spacing and b and by the decrease in energy of the torsional mode from 108 cm^{-1} to 102 cm^{-1}, relative to unheated muscovite (Table 2).

The creation of a trioctahedral dehydroxylated phase upon heating to 750 °C is somewhat more dubious because of its tendency to recrystallize (Brindley and Lemaitre, 1987). XRD indicates that high order (00l) reflections are still present in phlogopite and biotite upon heating to 750 °C, with their respective values of d_{001} becoming smaller. It is hard to avoid oxidation effects and, as Barshad and Kishk (1968) and Juo and White (1969) have shown, when Fe^{2+} is oxidized to Fe^{3+} upon heating, the redistribution of octahedral charge causes reorientation of the OH (Fig. 1). A subsequent decrease in the K-OH proton repulsion force is seen in XRD results by the decrease in d_{001} of both phlogopite and biotite. Phlogopite and biotite respond with increases in frequency of 3 cm^{-1} and 14 cm^{-1}, respectively. Biotite, which contains 25% FeO, displays the greatest oxidation effect (even under N_2 purged conditions). It also displays the greatest frequency shift. Frequency changes in trioctahedral micas caused by heating are therefore most likely attributable to oxidation-reduction reactions (i.e., OH reorientation rather than removal). The amount of change in frequency upon heating could potentially provide a rapid method for assessing thermally induced oxidation of Fe in the octahedral site.

Octahedral cation effects

A theoretical basis for the relation between ν_i and octahedral composition is partially supported from the data on OH and F substitution and OH orientation effects. Further examination for influences on the interlayer torsional mode is done through empirical testing of statistical significance in a multivariate analysis. Performing a regression analysis similar to that of Radoslovich (1962) for the b-cell parameter, using the potassium mica data from this study, reveals that the highest value of R^2 is achieved when only octahedral components are used as independent variables. As in Radoslovich's study, the correlation of tetrahedral Al with b is not found to be significant. Coefficients for the multiple regression, using octahedral components (including F) as independent variables, appear in Table 3. The correlation coefficient ($R^2 = 0.93$) indicates that the value of b can be predicted and, most importantly, substantiates the conclusions of

Table 3. Multiple regression analysis coefficients

Dependent variable	Octahedral ions							
	Constant	Al^{3+}	Fe^{3+}	Mg^{2+}	Fe^{2+}	Li^{+}	F^{-}	R^2
ν_i (cm^{-1})	79.6	7.61	9.09	0.96	−4.23	−4.65	2.20	0.99
b (Å)	9.183	−0.049	−0.083	0.015	0.050	−0.003	−0.022	0.93
d_{001} (Å)	10.041	−0.025	−0.054	0.012	0.028	−0.006	−0.032	0.92

Note: Octahedral cation proportions are expressed as 22 O equivalents per unit formula. Also, R^2 has been adjusted for small sample population (n = 12).

Radoslovich and Norrish (1962) on the importance of octahedral composition in controlling overall sheet dimensions.

Similar regression analysis using d_{001} as the dependent variable and octahedral components as independent variables reveals a relatively high correlation coefficient (R^2 = 0.92). Considering that the data are for potassium micas with a layer charge per unit formula of nearly −1, this correlation is not unexpected. In this case, the overall thickness of the structure reflects its composition.

Most revealing is the excellent correlation of octahedral composition with ν_i as the dependent variable (R^2 = 0.99). Trial-and-error regression analysis, similar to that used for the b, indicates that there is no statistically significant effect of tetrahedral Al. Using the coefficients from Table 3, a preliminary formula is presented and given as

$$\nu_i\ (cm^{-1}) = 79.6 + 0.96Mg^{2+} - 4.23Fe^{2+} + 7.61Al^{3+} + 9.09Fe^{3+} - 4.65Li^{+} + 2.20F^{-}. \quad (4)$$

Ion units are expressed as the number of octahedral cations assuming 22 O equivalents per unit formula. The significant standard coefficients of octahedral components support the idea that the environment of the interlayer K and basal O is largely influenced by the cations and F of the octahedral sheet. In addition to effects owing to F, the important effects of Li and Fe substitution (both Fe^{3+} for Al^{3+} and Fe^{2+} for Mg^{2+}) are demonstrated. The effect of increased mass in the octahedral sheet is increase in the octahedral sheet size (see, e.g., Tables 1 and 2 in Bailey, 1984). Low-frequency changes, concomitant with Fe substitution in trioctahedral potassium micas, can therefore be partially attributed to changes in the basal O environment that originate in response to changes within the octahedral sheet that are translated through the tetrahedral sheet.

Two distinct absorption bands (102 and 96 cm^{-1}) were observed for celadonite. This phenomenon has been observed for other celadonite samples and was first alluded to by Velde (1978). These two bands could result from several possible situations. The first possibility is a splitting caused by resonance of a fundamental torsional mode with an overtone of some lower-order vibrational mode. The lack of an observable band at about 50 cm^{-1} and the double mode behavior of other higher frequency bands suggests that this explanation is unlikely. A second possibility is the occurrence of two distinct torsional modes resulting from a heterogeneous octahedral charge distribution. Heterogeneities could arise either from a physical mixture of two similar, but different, celadonite structures within the same specimen or from the ordering of two octahedral environments within the same structure. The presence of two (060) reflections, using the preferred orientation technique, provides evidence for two similar, but different, celadonite structures present in this specimen, a phenomenon not uncommon to this family of micas (Buckley et al., 1978; Odom, 1984). Chemical formulae for celadonite suppose that a single 2:1 structural state and cations are apportioned into all possible sites. The heterogeneous octahedral cation distributions represented in the structural formula of Table 1 may therefore be an artifact in view of the fact that a mixture is present. In this study the two modes observed are interpreted as contributions from two phases with slightly different octahedral charge and mass distributions.

Lepidolite, which is similar to celadonite from the standpoint of having a heterogeneous octahedral charge distribution, also exhibits a double mode behavior. In contrast to celadonite, where there is little evidence to suggest long-range octahedral cation ordering, lepidolite does show long-range ordering (Guggenheim, 1981). Lepidolite from Ohio City, Colorado (Yale Peabody Museum B6489) has measured absorption bands at 100 and 94 cm^{-1}. Therefore, the double mode behavior of lepidolite can be inferred to arise from distinct K-O environments, influenced by distinct octahedral environments. The determination, based on absorption spectra alone, of whether double modes result from intracrystalline ordering or from physical mixtures of K-O environments can not be made at this time. However, it is clear that the torsional mode absorption region provides evidence for the presence of heterogeneous intrasheet structures.

The intermediate frequencies of the celadonite and lepidolite absorption bands relative to muscovite and phlogopite can be attributed to their di- or trioctahedral nature. Interestingly, the controls on the vibrational frequencies of celadonite and lepidolite are quite different. The intermediate frequencies of each suggests that net attractive forces between K and the OH and basal O are greater than those in phlogopite and biotite and less than those in muscovite. For Fe-rich celadonite the F content is low; consequently, F-related octahedral shortening effects appear to be unimportant. Celadonite differs from all other potassium micas studied by having the origin of its layer charge within the octahedral layer. The net effect

of octahedral charge distribution on OH orientations in celadonite is poorly constrained because detailed studies have not been carried out. The invariance of frequencies of celadonite upon heating provides some insight into the relative magnitude of OH orientation effects associated with di- and trioctahedral environments. Upon heating, it appears that the competing effects of OH reorientation (associated with Fe^{2+} oxidation) and dehydroxylation (associated with Fe^{3+} dioctahedral sites) on the vibrational frequency are of about the same magnitude. The increase in attractive forces between K and O of the OH and basal planes due to reorientation is equivalent to the decrease in forces between K and O of the basal and trivalent metal plane due to dehydroxylation.

The lower-frequency values for Fe-rich celadonite, relative to dioctahedral potassium micas, also can be attributed to the substitution of octahedral Fe^{3+} for Al^{3+}. The increase of overall octahedral sheet size in combination with tetrahedral sheets results in small amounts of tetrahedral sheet distortion (see α values in Table 2). The frequency of the torsional mode responds not only to the relative misfit of octahedral and tetrahedral sheets but also to the overall dimensions of the sheets. This latter relationship further accounts for the breakdown in agreement between α-refined values and α-calculated values, as proposed by Tateyama et al. (1977).

Lepidolite, in contrast to celadonite, typically exhibits significant amounts of substitution of F for OH. The combined effect of OH orientation not perpendicular to octahedral layers and F substitution is seen in the decrease in lattice parameters and in an increase in frequency relative to trioctahedral potassium micas. Each change reflects the increased attractive forces between K and octahedral F and K and basal tetrahedral O.

Conclusions

Naturally occurring potassium micas with a range in composition have been examined, utilizing the analytical techniques of far-IR spectroscopy, XRD and major oxide and F chemical analysis. The following relationships were found: (1) Substitutions of OH for F significantly affect torsional vibrational modes with increasing frequency accompanying increasing F concentration (a phenomenon primarily observed in trioctahedral structures). (2) Heating-induced dehydroxylation of dioctahedral species and heating-induced oxidation of Fe^{2+} trioctahedral species provide strong evidence for the control of OH orientation on the frequency of the interlayer torsional mode. (3) Multivariate statistical analysis of potassium mica intralayer sheet composition and the frequency of the interlayer torsional mode shows a strong correlation between the vibrational frequency of the K interlayer torsional mode and octahedral sheet composition. This relationship supports previous suggestions, based on XRD, that the sheet dimensions of layer-lattice silicates are controlled largely by the octahedral layer composition. (4) Multiple mode behavior provides evidence for heterogeneous K-basal O environments (controlled by octahedral site occupancy) in potassium micas; however, absorption spectra alone do not provide information about ordering of the environments.

Far-IR spectroscopy combined with X-ray diffraction provides a relatively rapid and simple analytical approach that gives direct information about the interlayer and octahedral environments of 2:1 phyllosilicates. The relationships between the structural and chemical parameters in micas, augmented by an understanding of controls on interlayer absorption bands, now potentially provides a basis for characterizing their clay mineral counterparts.

Acknowledgments

Financial support has been provided by an unrestricted grant-in-aid from Texaco Exploration and Production Technology Division, Houston, Texas, and GSA Research Grant no. 3870-87. Use of an IR spectrometer was kindly made available through Mike Herron and Mike Supp at the Schlumberger-Doll Research Laboratory in Ridgefield, Connecticut. The author benefited greatly from discussions with Rene Prost, Valarie Laperche, and Jim Howard. The editorial assistance of Bob Berner, Ellery Ingall, Tony Lasaga, Kathy Nagy, Philippe van Cappellen, Donald Peacor, and two anonymous reviewers is very much appreciated.

References cited

Bailey, S.W. (1984) Crystal chemistry of the true micas. In S.W. Bailey, Ed., Micas. Mineralogical Society of America Reviews in Mineralogy, 13, 13–60.

Barron, P.F., and Frost, R.L. (1984) Solid-state ^{29}Si and ^{27}Al nuclear magnetic resonance investigation of the dehydroxylation of pyrophyllite. Journal of Physical Chemistry, 88, 6206–6209.

Barshad, I., and Kishk, F.M. (1968) Oxidation of ferrous iron in vermiculite and biotite alters fixation and replaceability of potassium. Science, 162, 1401–1402.

Bodine, M.W., Jr. (1987) CLAYFORM: A fortran 77 computer program apportioning the constituents in the chemical analysis of a clay or other silicate mineral into a structural formula. Computers and Geosciences, 13, 77–88.

Bohlen, S.R., Peacor, D.R., and Essene, E.J. (1980) Crystal chemistry of a metamorphic biotite and its significance in water barometry. American Mineralogist, 65, 55–62.

Borg, I.Y., and Smith, D.K. (1969) Calculated X-ray powder patterns for silicate minerals. Geological Society of America Memoir 122, 896 p.

Brindley, G.W., and Lamaitre, J. (1987) Thermal, oxidation and reduction reactions in clay minerals. In A.C.D. Newman, Ed., Chemistry of clay minerals. Mineralogical Society Monograph 6, 319–370.

Buckley, H.A., Bevan, J.C., Brown, K.M., Johnson, L.R., and Farmer, V.C. (1978) Glauconite and celadonite: Two separate mineral species. Mineralogical Magazine, 42, 372–378.

Davis, J.C. (1986) Statistics and data analysis in geology. Wiley, New York, 646 p.

Eirish, M.V., and Tret'yakova, L.I. (1970) The role of sorptive layers in the formation and change of the crystal structure of montmorillonite. Clay Minerals, 8, 255–266.

Farmer, V.C. (1974) Layer silicates. In V.C. Farmer, Ed., Infrared spectra of minerals. Mineralogical Society Monograph 4, 331–360.

Franzini, M. (1969) The a and b micas layers and the crystal structure of sheet silicates. Contributions to Mineralogy and Petrology, 21, 203–224.

Frey, M., Hunziker, J.C., Jager, E., and Stern, W.B. (1983) Regional distribution of white K-mica polymorphs and their phengite content in the central Alps. Contributions to Mineralogy and Petrology, 83, 185–197.

Fripiat, J.J. (1982) Application of far infrared spectroscopy to the study of clay minerals and zeolites. In J.J. Fripiat, Ed., Developments in

sedimentology, v. 34: Advanced techniques for clay mineral analysis, p. 191–210. Elsevier, Amsterdam.

Gatineau, L. (1963) Localisation des replacements isomorphiques dans la muscovite. Comptes Rendus de l'Academie des Sciences de Paris, 256, 4648–4649.

Giese, R.F., Jr. (1971) Hydroxyl orientation in muscovite as indicated by electrostatic energy calculations. Science, 172, 263–264.

Guggenheim, S. (1981) Cation ordering in lepidolite. American Mineralogist, 66, 1221–1232.

Guidotti, C.V. (1984) Micas in metamorphic rocks. In S.W. Bailey, Ed., Micas. Mineralogical Society of America Reviews in Mineralogy, 13, 357–467.

Hazen, R.M., and Burnham, C.W. (1973) The crystal structures of one-layer phlogopite and annite. American Mineralogist, 58, 889–900.

Ishii, M., Shimanouchi, T., and Nakahira, M. (1967) Far infrared absorption of layer silicates. Inorganica Chimica Acta, 1, 387–392.

Juo, A.S.R., and White, J.L. (1969) Orientation of the dipole moments of hydroxyl groups in oxidized and unoxidized biotite. Science, 165, 804–805.

Laperche, V., and Prost, R. (1989) Far infrared study of compensating cations in clays. A.I.P.E.A. 9th International Clay Conference Abstracts with Program, Strasbourg, France, p. 224.

Leonard, R.A., and Weed, S.B. (1967) Influence of exchange ions on the *b*-dimensions of dioctahedral vermiculite. In Proceedings of the 15th Conference on Clays and Clay Minerals, 149–161.

Loh, E. (1973) Optical vibrations in sheet silicates. Journal of Physics C: Solid State Physics, 6, 1091–1104.

McCauley, J.W., and Newnham, R.E. (1971) Origin and prediction of ditrigonal distortions in micas. American Mineralogist, 56, 1626–1638.

Odom, I.E. (1984) Glauconite and celadonite minerals. In S.W. Bailey, Ed., Micas. Mineralogical Society of America Reviews in Mineralogy, 13, 545–572.

Prost, R., and Laperche, V. (1990) Far infrared study of potassium in micas. Clays and Clay Minerals, 38, 351–355.

Radoslovich, E.W. (1962) The cell dimensions and symmetry of layer-lattice silicates: II. Regression analysis. American Mineralogist, 47, 617–636.

Radoslovich, E.W., and Norrish, K. (1962) The cell dimensions and symmetry of layer-lattice silicates: I. Some structural considerations. American Mineralogist, 47, 599–616.

Rayner, J.H. (1974) The crystal structure of phlogopite by neutron diffraction. Mineralogical Magazine, 39, 850–856.

Roth, C. (1978) Effects of exchangeable cations on the far infrared spectra of clay minerals. In 6th International Clay Conference Abstracts with Program, 255 p.

Sanz, J., and Stone, W.E.E. (1983) NMR applied to minerals: IV. Local order in the octahedral sheet of micas: Fe-F avoidance. Clay Minerals, 18, 187–192.

Schroeder, P.A. (1989) Phyllosilicate sample mounting for far infrared absorption spectroscopy. A.I.P.E.A. 9th International Clay Conference Abstracts with Program, Strasbourg, France, p. 343.

Sidorenko, O.V., Zvyagin, B.B., and Soboleva, S.V. (1975) Crystal structure refinement for 1M dioctahedral mica. Soviet Physics: Crystallography, 20, 332–335.

Suquet, H., de la Calle, C., and Pezerat, H. (1975) Swelling and structural organization of saponite. Clays and Clay Minerals, 23, 1–9.

Takeda, H., and Morison, B. (1975) Comparison of observed and predicted structural parameters of mica at high temperatures. Acta Crystallographa, B31, 2444–2452.

Tateyama, H., Shimoda, S., and Sudo, T. (1977) Estimation of K-O distance and tetrahedral angle of K-micas from far-infrared absorption spectral data. American Mineralogist, 62, 534–539.

Thomas, J., Glass, H.D., White, W.A., and Trandel, R.M. (1977) Fluoride content of clay minerals and argillaceous earth materials. Clays and Clay Minerals, 25, 278–284.

Vedder, W., and MacDonald, R.S. (1963) Vibrations of the OH ions in muscovite. Journal of Chemical Physics, 38, 1583–1590.

Velde, B. (1978) Infrared spectra of synthetic micas in the series muscovite-MgAl celadonite. American Mineralogist, 63, 343–349.

Velde, B., and Couty, R. (1985) Far infrared spectra of hydrous layer silicates. Physical Chemistry of Minerals, 12, 347–352.

Wardle, R., and Brindley, G.W. (1972) The crystal structure of pyrophyllite, 1Tc and of its dehydroxylate. American Mineralogist, 57, 732–750.

Zhoukhlistov, A.P., Zvyagin, B.B., Lazarenko, E.K., and Pavlishin, V.I. (1977) Refinement of the crystal structure of ferrous seladonite. Soviet Physics: Crystallography, 22, 284–288.

Manuscript received December 27, 1989
Manuscript accepted August 1, 1990